Mitochondrial transfer to host cells from ex vivo expanded donor hematopoietic stem cells

Hiroki Kawano
University of Rochester School of Medicine and Dentistry
Yuko Kawano
University of Rochester School of Medicine and Dentistry
Charles O. Smith
University of Rochester School of Medicine and Dentistry
Mark W. LaMere
University of Rochester School of Medicine and Dentistry
Matthew J. McArthur
University of Rochester School of Medicine and Dentistry
Michael W. Becker
University of Rochester School of Medicine and Dentistry
Scott W. Ballinger
University of Alabama at Birmingham
Satoshi Gojo
Kyoto Prefectural University of Medicine
Roman A. Eliseev
University of Rochester School of Medicine and Dentistry
Laura M. Calvi (Laura_Calvi@urmc.rochester.edu)
University of Rochester School of Medicine and Dentistry

Article

Keywords:

Posted Date: April 28th, 2022

DOI: https://doi.org/10.21203/rs.3.rs-1585819/v1

Abstract

Mitochondrial dysfunction is observed in various conditions, from metabolic syndromes to mitochondrial diseases. Moreover, Mitochondrial DNA (mtDNA) transfer is an emerging mechanism that enables restoration of mitochondrial function in damaged cells. Hence, developing the technology that facilitates transfer of mtDNA can be a promising strategy for the treatment of these conditions. Here, we utilized an *ex vivo* culture of mouse hematopoietic stem cells (HSCs) and succeeded in expanding HSCs efficiently. Upon transplantation, sufficient donor HSC engraftment was attained in host. To assess the mitochondrial transfer via donor HSCs, we used mitochondrial-nuclear exchange (MNX) mice with nuclei from C57BL/6J and mitochondria from the C3H/HeN strain. Cells from MNX mice have C57BL/6J immunophenotype and C3H/HeN mtDNA, which is known to confer a higher stress resistance to mitochondria. *Ex vivo* expanded MNX HSCs were transplanted into irradiated C57BL/6J mice and the analyses were done at six weeks post transplantation. We observed high engraftment of donor cells in peripheral blood as well as in bone marrow. We also found that HSCs from the MNX mice could transfer mtDNA to host cells. This work highlights the utility of *ex vivo* expanded HSC to achieve the mitochondrial transfer from donor to host in the transplant setting.

Introduction

Mitochondria are highly dynamic organelles that regulate cell bioenergetics and fluxes of key metabolites and ions [1]. Their diverse functions are regulated by fission and fusion machinery, factors controlling biogenesis, ion transport, quality control mechanisms such as autophagy/mitophagy, and other factors [2]. Mitochondrial impairment has been shown to play a role in various pathophysiologic states, including organ dysfunctions due to degenerative changes, metabolic syndromes like diabetes, aging, sustained chronic inflammation, space flight and cancers[3 4,5]. There is also a range of mitochondrial diseases caused by mutations in the nuclear DNA- or mitochondrial DNA (mtDNA)-encoded mitochondrial genes, such as the Leigh syndrome and other conditions [6]. Various approaches have been used to elucidate the effects of mitochondria and mtDNA on biological processes, particularly multi-factorial events such as cancer and aging. Higher vulnerability of the mitochondrial genome to ethidium bromide relative to the nuclear genome has long been used to eliminate the mitochondrial genome, and cells that have been exposed to ethidium bromide and have lost their mitochondria are called ρ0 cells [7]. Fusion of the ρ0 cell and enucleated cell is called a cybrid cell, and it has played an extremely important role in studying the involvement of the mitochondrial genome in the cancer field [8]. On the other hand, the use of cybrid cells is hampered by the fact that the effects of the carcinogenic properties of ethidium bromide on the nuclear genome cannot be ruled out. Taking advantage of the fact that the mitochondrial genome is maternally inherited, mice called conplastic mice have also elicited significant findings in aging and other areas [9]. To create these mice, the male lineage is fixed and offspring born to its male lineage is used as female, and the offspring female is crossed with that male lineage again. By continuing this process, a new combination of mitochondrial and nuclear genomes can be created, with the mitochondrial genome derived from the female and the nuclear genome from the male [10]. On the other hand, using assisted

reproductive technology, a new mitochondrial genome/nucleus genome combination can be created using nuclear transplantation, generating mitochondria nuclear exchange (MNX) mice [11]. A large time saving compared to conplastic mice has been achieved this way. A number of results have been reported using MNX mice, including that the mitochondrial genome alters the cancer microenvironment and alters metastatic potential [12], that it alters immune cell differentiation [13], and that the molecular mechanism underlying their phenotypic change is the alteration of the nuclear epigenome through mitochondrial intermediate metabolites [14].

Recently, the evidence has been accumulating that mitochondrial transfer occurs in different cell types both *in vitro* and *in vivo* [15], in which donor cells, e.g. mesenchymal stem cells (MSCs), transfer mitochondria to other cells [16]. Many studies suggest that mitochondrial transfer can help the recovery process in injured cells or tissues [17]. MSCs have been evaluated as a practical source of mitochondrial transfer in the regenerative treatment for deteriorated kidney in diabetes [18]or damaged cerebrovascular system in strokes [19]. However, other primary cells, such as HSCs, have not been fully explored as a source of mitochondrial transfer. Hematopoietic stem cells (HSCs) are multipotent self-renewing cells that regenerate the blood system after transplantation [20]. However, until recently, we lacked the technology to efficiently expand HSCs *ex vivo* until the development of a novel system where the culture media is supplemented with the unique replacement for serum albumin, polyvinyl alcohol (PVA) [21–23]. This novel technology can potentially enable us to manipulate primary HSCs ex vivo.

In this work, we have thoroughly evaluated the *ex vivo* expansion of mouse HSCs from young or middle-aged mice. We present our data indicating reproducible quality of the *ex vivo* culture of HSCs and that the culture from middle-aged mice shows the preserved functional HSCs, demonstrated utilizing the lethally irradiated transplant model [24]. We also identified mitochondrial transfer from donor HSCs to host cells by analyzing mtDNA in each population after transplant utilizing MNX mice, which possesses C57BL/6J (C57) nuclear and C3H/HeN (C3H) mitochondrial DNA [11]. These mice have C57 immunophenotype and thus cells from the MNX mice can be safely transplanted into the C57 hosts without triggering any immune response. Notably, mitochondria in these MNX mice inherit the bioenergetic economy of the C3H strain when compared to the C57 strain [11]. We, therefore hypothesized that the more resistant mitochondria of the donor MNX cells will have high chances of transfer into the less resistant C57 host cells.

Results

Ex vivo **culture of mouse HSCs from young mice reveals robust expansion pattern and reserved functional HSCs in the transplant assay**

To establish and confirm the reproducibility of *ex vivo* culture of mouse HSCs, we first harvested bone marrow from young mice and isolated HSCs according to the previously reported protocol [22]. The recent report also implies that even minor differences in culture constitutes can affect the maintenance of HSC

in vitro[22,23]. In our experience, intense monitoring of cell morphology was required to time media changes. We used alternative culture media that are also described as optional by Wilkinson et al [22](see Methods). Moreover, we found that a stringent cKit + Sca1 + lineage- (KSL)CD150 + CD34- gate was needed to sort an HSC population that would expand *ex vivo* in this culture conditions and to avoid the contamination of hematopoietic progenitor cells. The percent of each gating population was almost similar to that of previously described (Fig. 1). The expansion of both total and KSL cell population was achieved very efficiently as assessed by flow cytometry (Fig. 2a). The morphology of cells in culture was consistent with previous report, in which small cells are dominant with some large cells, thought to be megakaryocytes (arrowhead), present (Fig. 2b). To evaluate the presence of functional HSCs, we performed conditional transplant utilizing lethal irradiation. We injected increasing doses of CD45.2BL6 HSCs into CD45.1 ubiquitin C/green fluorescent protein (UBC/GFP) recipient mice, which gave us the opportunity to evaluate the composition of HSC/ hematopoietic progenitor cell (HPC) or bone marrow mature cells based on both CD45 subtype and GFP positivity (Fig. 2c). The engraftment of donor cells in peripheral blood or bone marrow improved in a cell number-dependent manner (Fig. 2d). The complete blood counts (CBCs) of recipient mice indicated hematopoietic reconstitution by donor cells, which was also compatible with high donor engraftment in bone marrow at 16 weeks (Fig. 2e). For further evaluation of donor cell presence in the bone marrow, we analyzed whole bone marrow with flow cytometry based on the approach we previously described [25].

Ex vivo expanded mouse HSCs efficiently replaced host hematopoietic progenitor cells (HPCs) or HSCs in donor cell number-dependent manner.

The bone marrow cells were analyzed in the recipient mice 16 weeks after transplantation. The donor or recipient cells were clearly separated by flow cytometry based on GFP expression. Each HPC/HSC population was dominated by donor-derived cells. Donor cell titration revealed the dose dependent increases of donor engraftment (Fig. 3a). Consistent with HSC differentiation, the composition of mature cells in the bone marrow also showed the predominance of donor-derived cells as was seen in the HPC/HSC compartment (Fig. 3b). The chimerism of donor cells was relatively low in T cells, which suggests the presence of residual persistent recipient T cells.

The ex vivo HSC culture from middle-aged MNX mice remained highly enriched in CD150 + HSCs with high potential of engraftment after transplantation.

Next, we assessed the *ex vivo* HSC culture utilizing 10 months-old MNX mice. As was described above, MNX mice have C57 nuclear genome and C3H mtDNA [11]. Since C3H and C57 mtDNA have different genetic markers easily identified via PCR and restriction digest [11], this system allows convenient detection of donor C3H mtDNA in GFP + C57 host cells. As expected from middle aged mice, MNX mice had increased In KSL and CD150 + HSC populations (Fig. 4, Gate 7 and Gate 8) compared to HSCs from young donors (Fig. 1, Gate 7 and Gate 8). Evaluation of *ex vivo* culture after sorting HSCs revealed high retention of CD150 + KSL populations in the culture (Fig. 5) with a growth pattern comparable to that seen in young HSCs (Fig. 5). We then injected $5x10^5$ *ex vivo* expanded MNX HSCs into lethally irradiated

CD45.1 UBC/GFP (C57 background) recipient mice (Fig. 6a). Since we expected that mitochondrial transfer would occur at early time points after the transplantation, we analyzed recipient mice at 6 weeks, which is an early time point when hematopoietic engraftment should have stabilized. Consistent with this, CBC data revealed complete recovery by 6 weeks post transplantation (Fig. 6c). Therefore, at six weeks post transplantation, we harvested bone marrow and spleens for further evaluation of mitochondrial transfer from MNX donor cells to recipient cells. The chimerism in each tissue was very high, especially in the bone marrow (Fig. 6b). In parallel with this, we found that HPC/HSCs in the bone marrow were highly replaced with donor-derived cells and each population cell number was comparable with the non-transplant age- and sex-matched mice (Fig. 7a), which implies robust reconstitution capacities of donor cells *in vivo*. Furthermore, the donor cell distribution in mature bone marrow population was consistent with this (Fig. 7b).

mtDNA transfer from donor to host in a transplant model utilizing ex vivo **expanded mouse HSC culture.**

To investigate the potential of donor HSCs to transfer their mitochondria and, thus, mtDNA to the host, we have extracted cells from bone marrow and spleens of the recipient mice for mtDNA analysis. As described above, the recipient mice were of C57 background while the donor HSCs were from MNX (C57 nucleus and C3H mtDNA). The *mt-Co3* gene of C57 mice carries a SNP that forms *Pflf1* restriction site and thus, can be cleaved with the restriction enzyme *Pflf1*, while that of C3H cannot. On the other hand, the *mt-Nd3* gene of C3H mice carries a SNP that forms *Bcl1* restriction site and thus, can be cleaved by the restriction enzyme *Bcl1*, while that of C57 cannot. By observing the different bands generated by digesting mtDNA with these restriction enzymes, we can trace the origin of the mitochondrial genome. We separated GFP- donor cells and GFP + host cells via sorting. However, we could not attain the DNA analysis in GFP + cells in the bone marrow due to the extremely low frequency of these cells. From the spleen, we received sufficient numbers of both donor (GFP-) and host (GFP+) cells. With a distinct separation of GFP- and GFP + cells in spleens, we have found that the donor C3H mtDNA was transferred to the GFP + host cells (Fig. 8a). In particular, after PCR amplification of either *mt-Co3* or *mt-Nd3* gene fragments and digest of these fragments with either *Pflf1* or *Bcl1* respectively, the host GFP + cells showed three bands (one uncut wild type band and two cut products from SNP-carrying), suggesting that the donor (C3H) mitochondrial genome coexists in the recipient cells with the recipient (C57) mitochondrial genome. The reverse transfer of mtDNA from recipient to donor was also detected but to a much lower extent, which suggests bi-directionality of mitochondrial transfer (Fig. 8b).

Discussion

In the current study, we have demonstrated that *ex vivo* expansion of mouse HSCs can be attained with the careful monitoring and sorting approach gating KSL cell population. We also observed that the donor to host mitochondrial transfer occurred in recipient mice transplanted with HSCs from this culture system. HSC culture *ex vivo* has been intensely explored due to the necessity of HSCs for basic research as well as in clinical aspects. This is despite the difficulties of maintaining HSCs while preventing cell differentiation into mature cells. Takubo et al has developed an *in vitro* conditioning system to maintain

the quiescent HSC in culture under low cytokines concentrations of stem cell factor (SCF) and thrombopoietin (TPO), hypoxia, and high amounts of fatty acid, with which they attained 30–40% donor chimerism at four months after transplantation [26]. Wilkinson et al have utilized PVA to replace serum albumin in mouse HSC in *ex vivo* culture to avoid the contamination of cytokines that induce differentiation of HSCs [21,22]. This approach has shown long-term stable expansion of functional HSCs *ex vivo* and sufficient engraftment capacity *in vivo*. Our culture following the protocol by Wilkinson showed relatively rapid HSC growth to reach subconfluency in 2 weeks, which is comparable to their result (8133x increase on day 28). However, very efficient engraftment or expected HSC number in vitro have been observed, which suggests that *ex vivo* HSC expansion pattern can vary possibly depending on multiple factors including the culture condition and gating strategy of HSCs. Although the trafficking of exogenous mitochondria associated with their transfer has been reported through tunneling nanotube either *in vitro* [27] or *in vivo* [28], and trafficking vesicles, such as exosome [17] and exopher [29], the phenomenon of mitochondrial substitution has never been recognized in the context of mitochondrial transfer. Mitochondrial diseases, especially those caused by mutations in the mitochondrial genome, are still rare intractable diseases for which there is no cure [30]. In recent years, significant progress in genome editing technology has led to the proposal of methods to modify the genome by up to 50%, targeting mutations with point mutations [31]. Mitochondrial genome mutations do not develop phenotypic alternations until a certain threshold is crossed, and there are cases where mitochondrial genome mutations cross the threshold and phenotypically develop when a child is delivered from a mother of a carrier. Assisted reproductive technology has developed a mitochondrial replacement method that applies nuclear transfer to establish fertilization with the mother's nucleus with third-party oocyte cytoplasm and the father's sperm [32], and has already reached clinical practice [33]. However, even with this elaborated technique, a re-dominance, or reversion, of the residual, slightly mutated mitochondrial genome of maternal origin has been observed [34]. The protocol that has made this mitochondrial genome replacement possible in somatic cells, whereby mitochondrial genomes are reduced once and then internalization of isolated mitochondria is promoted, has been reported to result in complete mitochondrial genome replacement in most cells [35]. Unlike these previous reports, in the current study, we demonstrate mitochondrial genome replacement in the setting of transplantation, where there is mixing of donor and recipient cells. Although it is completely unknown how heteroplasmy, which represents the heterogeneity of the mitochondrial genome, is regulated [36], methods to modulate heteroplasmy would greatly contribute to the development of treatment strategies for mitochondrial diseases for which currently no treatment methods exist.

Some reports suggest that intercellular mitochondrial transfer occurs under both physiological and pathological conditions via donor cells, including MSC or astrocytes. This phenomenon potentially contributes to maintaining homeostasis or supporting recovery after tissue injury [37]. Despite the limitation of attaining sufficient number of host cells in a transplant model, we were clearly able to detect the mitochondrial transfer from donor cells to host cells in spleen utilizing *ex vivo* expansion culture

systems, demonstrating the ability of HSCs and their progeny to donate mitochondria, even after *ex vivo* expansion.

Golan et al have recently revealed that CD45 + donor cells contribute to mitochondrial transfer to bone marrow MSCs via cell-cell contact for the recovery from the irradiation-associated damages in conditional mouse transplant [38]. Interestingly, they also found opposite mitochondrial transfer from recipient to donor HSCs utilizing Dendra2-mitochondria transgenic mice [39], which is consistent with our finding utilizing highly purified HSC cells in *ex vivo* culture. Collectively, these findings suggest the complex bi-directional interactions between donor and recipient hematopoietic stem and progenitor cells (HSPCs) as well as bone marrow mitochondrial cells that occur to reconstitute hematopoietic system. While the transfer of mitochondria and, therefore, mitochondrial genomes following hematopoietic stem cell transplantation was previously reported [40], this exchange occurs in the bone marrow, where donor cells have been engrafted. In the present study, however, we found that progenies differentiated from transplanted stem cells could supply mitochondria to the recipient cells in the spleen, suggesting the possibility that mitochondrial trafficking can occur not only in the bone marrow but also in remote organs following hematopoietic stem cell transplantation. To our knowledge, this is the first report of this occurrence. Whether this transfer can also occur in other key organ, such as liver and/or muscle, should be examined in future studies.

Mitochondria, involved not only in energy metabolism but also in epigenome-mediated regulation of cell differentiation [41] and intracellular innate immunity [42], are intercellularly more dynamic than ever thought possible. It would be of great impact to elucidate how mitochondria move between cells, what kind of cells perform this trafficking and by what mechanism. Our current study opens the door for future investigation of these mechanisms.

In summary, we have evaluated and confirmed robust expansion of mouse HSCs *ex vivo*. This culture system, while requiring careful monitoring and optimization of culture constituents, has the potential for broad range of applications in HSC research. We have also established that using this technology enables us to demonstrate mitochondrial transfer between donor and recipient cells. Our results suggest that this can potentially be a novel approach for understating the remodeling of the bone marrow microenvironment after transplantation, and may represent a novel therapeutic strategy to mitigate not only mitochondrial diseases, but also cancer and neurodegenerative diseases where mitochondrial genome and dynamics are disrupted.

Methods

Study approval.

All murine studies were performed in accordance with protocols approved by the Institutional Animal Care and Use Committee, the University Committee on Animal Resources (University of Rochester, Rochester, New York, USA). This study was performed in accordance with ARRIVE guidelines.

Mice.

Mice were maintained within the Vivarium facility at the University of Rochester School of Medicine and Dentistry in accordance with protocols approved by the Institutional Animal Care and Use Committee. C57BL/6J were purchased from The Jackson Laboratory and bred in house. All strains were of the C57BL/6J background and expressed the CD45.2. Strains used include C57BL/6J, PepBoy CD45.1 (B6.SJL-*Ptprc*^{a} *Pepc*^{b}/BoyJ), *UBC-GFP* (*C57BL/6-Tg (UBC-GFP) 30Scha/J*), and MNX (C57BL/6-MNX: C57n;C3Hmt) originated in the laboratory of Dr Scott Ballinger (U of Alabama at Birmingham).

Complete blood counts.

Blood was collected from the submandibular plexus and collected in EDTA-coated tubes. The scil Vet abc Plus + was used to analyze complete blood counts, as we previously published [25].

Light microscopy.

Images were taken at room temperature using an Olympus CKX41 microscope, Olympus DP74 camera. Cellsens software (Olympus) was used to acquire images on the microscope.

Flow cytometry.

Analysis of marrow cell populations was done as previously described [25]. For marrow cell analysis, marrow was released by crushing with a mortar and pestle in 1x PBS. Analysis for hematopoietic, and mature cell populations was performed as previously described [43]. Samples were run on a BD LSR Fortessa flow cytometer: 5 lasers, UV (355 nm), violet (405 nm), blue (488 nm), yellow-green (561 nm), and red (640 nm) lasers (BD Biosciences). As a dead stain, DAPI was used. Analysis was performed using FCS Express version 7 (De Novo Software). The gating strategy used to identify populations enriched for cells of interest has been previously described [22]. Sorting was done on a FACSAria with 405-, 488-, 532- and 640-lasers (BD Biosciences).

HSC isolation by fluorescence-activated cell sorting.

Ex vivo mouse HSC collection was done as previously described [21]. Briefly, mouse bone-marrow cells were isolated from the tibia and femur, stained with APC-c-Kit antibody. C-kit positive cells were enriched using anti-APC magnetic beads with auto MACS pro (Miltenyi Biotec). The c-Kit-enriched cells were subsequently stained with a lineage antibody cocktail (biotinylated CD3, TER119, LY-6G/LY-6C, and B220), anti-CD11b, anti-CD34, anti-Sca1, and anti-CD150 before being stained with streptavidin APC for 60 min. Antibodies used are listed in Supplementary Table S1. Cell populations were then purified using a FACS Aria and plated into the designated plate. Isolation and analyses were performed using serum free PBS.

HSC ex vivo culture.

Purified HSC cells were cultured in serum-free medium with PVA, HemEX-Type9A medium (Cell Science Technology Institute, A5P00P01C) supplemented with 1% P/S (Gibco), 100ng/ml mouse TPO (Peprotech), 10 ng/ml mouse SCF (Peprotech) at 37°C with 5% CO_2. Complete medium changes were made every 2 days after the first 3 days as described [21]. All the cultures were performed utilizing flat-bottomed plates, tissue-culture-treated coated with fibronectin (Corning).

Quality tests of cultured cells.

Following *ex vivo* culture, cells were manually counted using hemocytometer. For flow cytometric analysis, cells were stained with antibodies described in supplemental Table for 30 min. Following a wash step, the cells were run with a flow cytometry as mentioned above.

Transplant assays.

For non-competitive transplants, $5x10^5$ *ex vivo* expanded donor HSC cells were intravenously injected via the tail vein into recipient mice. Recipient mice were conditioned with a lethal dose of radiation using a ^{137}Cs source (2 doses of 6 Gy total body irradiation, first at 24hr prior and the second at 1-3hrs prior to transplantation).

Detection of C3H and C57 mtDNA.

This was done according to the previously published protocol [11] using specific PCR probes, PCR, and subsequent restriction digest. Briefly, viable donor (GFP-) and recipient (GFP+) cells were sorted and DNA extracted using the Wizard SV DNA kit (Promega). C3H mouse mtDNA carries a SNP in the *mtNd3* gene forming a *Bcl1* restriction site. To detect C3H mtDNA, we amplified the region carrying this restriction site using the following primers: 5'-TTC CAA TTA GTA GAT TCT GAA TAA ACC CAG AAG AGA GTG AT-3' and 5'-AAA TTT TAT TGA GAA TGG TAG ACG-3'. PCR was done and the product cut with *Bcl1*. The C3H mtDNA is cleaved into 166 bp and 38 bp fragments, while the C57 mtDNA remains uncut.

C57 mouse mtDNA carries a SNP in the *mtCo3* gene forming a *Pflf1* restriction site. To detect C57 mtDNA, we amplified the region carrying this restriction site using the following primers: 5'-CGA AAC CAC ATA AAT CAA GCC C-3' and 5'-CTC TCT TCT GGG TTT ATT CAG A-3'. PCR was done and the product cut with *Pflf1*. The C57 mtDNA is cleaved into 274 bp and 111 bp fragments while the C3H mtDNA remains uncut.

Statistical analysis.

All data are reported as mean ± standard error of the mean. All analyses were made with GraphPad Prism software (version 9) using 2-tailed Student's *t* test, Mann-Whitney nonparametric testing, or 1-way ANOVA with Tukey's multiple-comparisons post-test when appropriate. A *P* value less than 0.05 was considered significant and denoted by asterisks (*$p < 0.05$, **$p < 0.01$, ***$p < 0.001$).

Declarations

Acknowledgements

We thank members of the Calvi laboratory for discussion: Lizz LaMere and Daniel Byunfor experimental support; and the University of Rochester Flow Cytometry for their assistance. Funding for this work was provided by IMEL Biotherapeutics. This work was also supported by the National Institutes of Health grant P30 AR061307 and the Edward P Evans Foundation grant #005545 (to L.M.C).

Author contributions

H.K., Y.K, R.E., L.C. designed the study, analyzed the data, and wrote the paper. C.S., M.L., M.M, M.B, S.B., and S.G. contributed to the interpretation of data.

Competing interests

The authors declare no competing interests.

Additional information

Supplementary information is available for this paper.

Correspondence and requests for materials should be addressed to R.E. and L.C.

Availability of Data and Materials

The datasets used and/or analysed during the current study available from the corresponding authors on reasonable request.

References

1. Mishra, P. & Chan, D. C. Mitochondrial dynamics and inheritance during cell division, development and disease. *Nature reviews. Molecular cell biology* **15**, 634-646, doi:10.1038/nrm3877 (2014).
2. Detmer, S. A. & Chan, D. C. Functions and dysfunctions of mitochondrial dynamics. *Nature reviews. Molecular cell biology* **8**, 870-879, doi:10.1038/nrm2275 (2007).
3. da Silveira, W. A.*et al.* Comprehensive Multi-omics Analysis Reveals Mitochondrial Stress as a Central Biological Hub for Spaceflight Impact. *Cell* **183**, 1185-1201 e1120, doi:10.1016/j.cell.2020.11.002 (2020).
4. Geto, Z., Molla, M. D., Challa, F., Belay, Y. & Getahun, T. Mitochondrial Dynamic Dysfunction as a Main Triggering Factor for Inflammation Associated Chronic Non-Communicable Diseases. *Journal of inflammation research* **13**, 97-107, doi:10.2147/JIR.S232009 (2020).
5. Giang, A. H.*et al.* Mitochondrial dysfunction and permeability transition in osteosarcoma cells showing the Warburg effect. *The Journal of biological chemistry* **288**, 33303-33311,

doi:10.1074/jbc.M113.507129 (2013).

6. Ng, Y. S.*et al.* Mitochondrial disease in adults: recent advances and future promise. *The Lancet. Neurology* **20**, 573-584, doi:10.1016/S1474-4422(21)00098-3 (2021).
7. King, M. P. & Attardi, G. Human cells lacking mtDNA: repopulation with exogenous mitochondria by complementation. *Science* **246**, 500 (1989).
8. Ishikawa, K.*et al.* ROS-generating mitochondrial DNA mutations can regulate tumor cell metastasis. *Science* **320**, 661-664 (2008).
9. Latorre-Pellicer, A.*et al.* Mitochondrial and nuclear DNA matching shapes metabolism and healthy ageing. *Nature* **535**, 561-565, doi:10.1038/nature18618 (2016).
10. Gusdon, A. M., Votyakova, T. V., Reynolds, I. J. & Mathews, C. E. Nuclear and mitochondrial interaction involving mt-Nd2 leads to increased mitochondrial reactive oxygen species production. *J Biol Chem* **282**, 5171-5179, doi:10.1074/jbc.M609367200 (2007).
11. Kesterson, R. A.*et al.* Generation of Mitochondrial-nuclear eXchange Mice via Pronuclear Transfer. *Bio-protocol* **6**, doi:10.21769/BioProtoc.1976 (2016).
12. Brinker, A. E.*et al.* Mitochondrial Haplotype of the Host Stromal Microenvironment Alters Metastasis in a Non-cell Autonomous Manner. *Cancer Res* **80**, 1118-1129, doi:10.1158/0008-5472.CAN-19-2481 (2020).
13. Beadnell, T. C.*et al.* Mitochondrial genetics cooperate with nuclear genetics to selectively alter immune cell development/trafficking. *Biochim Biophys Acta Mol Basis Dis* **1866**, 165648, doi:10.1016/j.bbadis.2019.165648 (2020).
14. Vivian, C. J.*et al.* Mitochondrial Genomic Backgrounds Affect Nuclear DNA Methylation and Gene Expression. *Cancer Res* **77**, 6202-6214, doi:10.1158/0008-5472.CAN-17-1473 (2017).
15. Liu, F., Lu, J., Manaenko, A., Tang, J. & Hu, Q. Mitochondria in Ischemic Stroke: New Insight and Implications. *Aging and disease* **9**, 924-937, doi:10.14336/AD.2017.1126 (2018).
16. Spees, J. L., Olson, S. D., Whitney, M. J. & Prockop, D. J. Mitochondrial transfer between cells can rescue aerobic respiration. *Proceedings of the National Academy of Sciences of the United States of America* **103**, 1283-1288, doi:10.1073/pnas.0510511103 (2006).
17. Hayakawa, K.*et al.* Transfer of mitochondria from astrocytes to neurons after stroke. *Nature* **535**, 551-555, doi:10.1038/nature18928 (2016).
18. Konari, N., Nagaishi, K., Kikuchi, S. & Fujimiya, M. Mitochondria transfer from mesenchymal stem cells structurally and functionally repairs renal proximal tubular epithelial cells in diabetic nephropathy in vivo. *Scientific reports* **9**, 5184, doi:10.1038/s41598-019-40163-y (2019).
19. Liu, K., Guo, L., Zhou, Z., Pan, M. & Yan, C. Mesenchymal stem cells transfer mitochondria into cerebral microvasculature and promote recovery from ischemic stroke. *Microvascular research* **123**, 74-80, doi:10.1016/j.mvr.2019.01.001 (2019).
20. Osawa, M., Hanada, K., Hamada, H. & Nakauchi, H. Long-term lymphohematopoietic reconstitution by a single CD34-low/negative hematopoietic stem cell. *Science* **273**, 242-245,

doi:10.1126/science.273.5272.242 (1996).

21. Wilkinson, A. C.*et al.* Long-term ex vivo haematopoietic-stem-cell expansion allows nonconditioned transplantation. *Nature* **571**, 117-121, doi:10.1038/s41586-019-1244-x (2019).
22. Wilkinson, A. C., Ishida, R., Nakauchi, H. & Yamazaki, S. Long-term ex vivo expansion of mouse hematopoietic stem cells. *Nature protocols* **15**, 628-648, doi:10.1038/s41596-019-0263-2 (2020).
23. Sudo, K., Yamazaki, S., Wilkinson, A. C., Nakauchi, H. & Nakamura, Y. Polyvinyl alcohol hydrolysis rate and molecular weight influence human and murine HSC activity ex vivo. *Stem cell research* **56**, 102531, doi:10.1016/j.scr.2021.102531 (2021).
24. Suzuki, T.*et al.* Mobilization efficiency is critically regulated by fat via marrow PPARdelta. *Haematologica* **106**, 1671-1683, doi:10.3324/haematol.2020.265751 (2021).
25. Frisch, B. J.*et al.* Aged marrow macrophages expand platelet-biased hematopoietic stem cells via Interleukin1B. *JCI Insight* **5**, doi:10.1172/jci.insight.124213 (2019).
26. Kobayashi, H.*et al.* Environmental Optimization Enables Maintenance of Quiescent Hematopoietic Stem Cells Ex Vivo. *Cell reports* **28**, 145-158 e149, doi:10.1016/j.celrep.2019.06.008 (2019).
27. Rustom, A., Saffrich, R., Markovic, I., Walther, P. & Gerdes, H. H. Nanotubular highways for intercellular organelle transport. *Science* **303**, 1007-1010, doi:10.1126/science.1093133 (2004).
28. Saha, T.*et al.* Intercellular nanotubes mediate mitochondrial trafficking between cancer and immune cells. *Nat Nanotechnol*, doi:10.1038/s41565-021-01000-4 (2021).
29. Nicolas-Avila, J. A.*et al.* A Network of Macrophages Supports Mitochondrial Homeostasis in the Heart. *Cell* **183**, 94-109 e123, doi:10.1016/j.cell.2020.08.031 (2020).
30. Gorman, G. S.*et al.* Mitochondrial diseases. *Nat Rev Dis Primers* **2**, 16080, doi:10.1038/nrdp.2016.80 (2016).
31. Mok, B. Y.*et al.* A bacterial cytidine deaminase toxin enables CRISPR-free mitochondrial base editing. *Nature* **583**, 631-637, doi:10.1038/s41586-020-2477-4 (2020).
32. Tachibana, M.*et al.* Mitochondrial gene replacement in primate offspring and embryonic stem cells. *Nature* **461**, 367-372, doi:10.1038/nature08368 (2009).
33. Greenfield, A.*et al.* Assisted reproductive technologies to prevent human mitochondrial disease transmission. *Nat Biotechnol* **35**, 1059-1068, doi:10.1038/nbt.3997 (2017).
34. Kang, E.*et al.* Mitochondrial replacement in human oocytes carrying pathogenic mitochondrial DNA mutations. *Nature* **540**, 270-275, doi:10.1038/nature20592 (2016).
35. Maeda, H., Kami, D., Maeda, R., Shikuma, A. & Gojo, S. Generation of somatic mitochondrial DNA-replaced cells for mitochondrial dysfunction treatment. *Sci Rep* **11**, 10897, doi:10.1038/s41598-021-90316-1 (2021).
36. Stewart, J. B. & Chinnery, P. F. The dynamics of mitochondrial DNA heteroplasmy: implications for human health and disease. *Nat Rev Genet* **16**, 530-542, doi:10.1038/nrg3966 (2015).
37. Liu, D.*et al.* Intercellular mitochondrial transfer as a means of tissue revitalization. *Signal transduction and targeted therapy* **6**, 65, doi:10.1038/s41392-020-00440-z (2021).

38. Golan, K.*et al.* Bone marrow regeneration requires mitochondrial transfer from donor Cx43-expressing hematopoietic progenitors to stroma. *Blood* **136**, 2607-2619, doi:10.1182/blood.2020005399 (2020).
39. Pham, A. H., McCaffery, J. M. & Chan, D. C. Mouse lines with photo-activatable mitochondria to study mitochondrial dynamics. *Genesis* **50**, 833-843, doi:10.1002/dvg.22050 (2012).
40. Moschoi, R.*et al.* Protective mitochondrial transfer from bone marrow stromal cells to acute myeloid leukemic cells during chemotherapy. *Blood* **128**, 253-264, doi:10.1182/blood-2015-07-655860 (2016).
41. Matilainen, O., Quiros, P. M. & Auwerx, J. Mitochondria and Epigenetics - Crosstalk in Homeostasis and Stress. *Trends Cell Biol* **27**, 453-463, doi:10.1016/j.tcb.2017.02.004 (2017).
42. Mills, E. L., Kelly, B. & O'Neill, L. A. J. Mitochondria are the powerhouses of immunity. *Nat Immunol* **18**, 488-498, doi:10.1038/ni.3704 (2017).
43. Balderman, S. R.*et al.* Targeting of the bone marrow microenvironment improves outcome in a murine model of myelodysplastic syndrome. *Blood* **127**, 616-625, doi:10.1182/blood-2015-06-653113 (2016).

Figures

Figure 1.

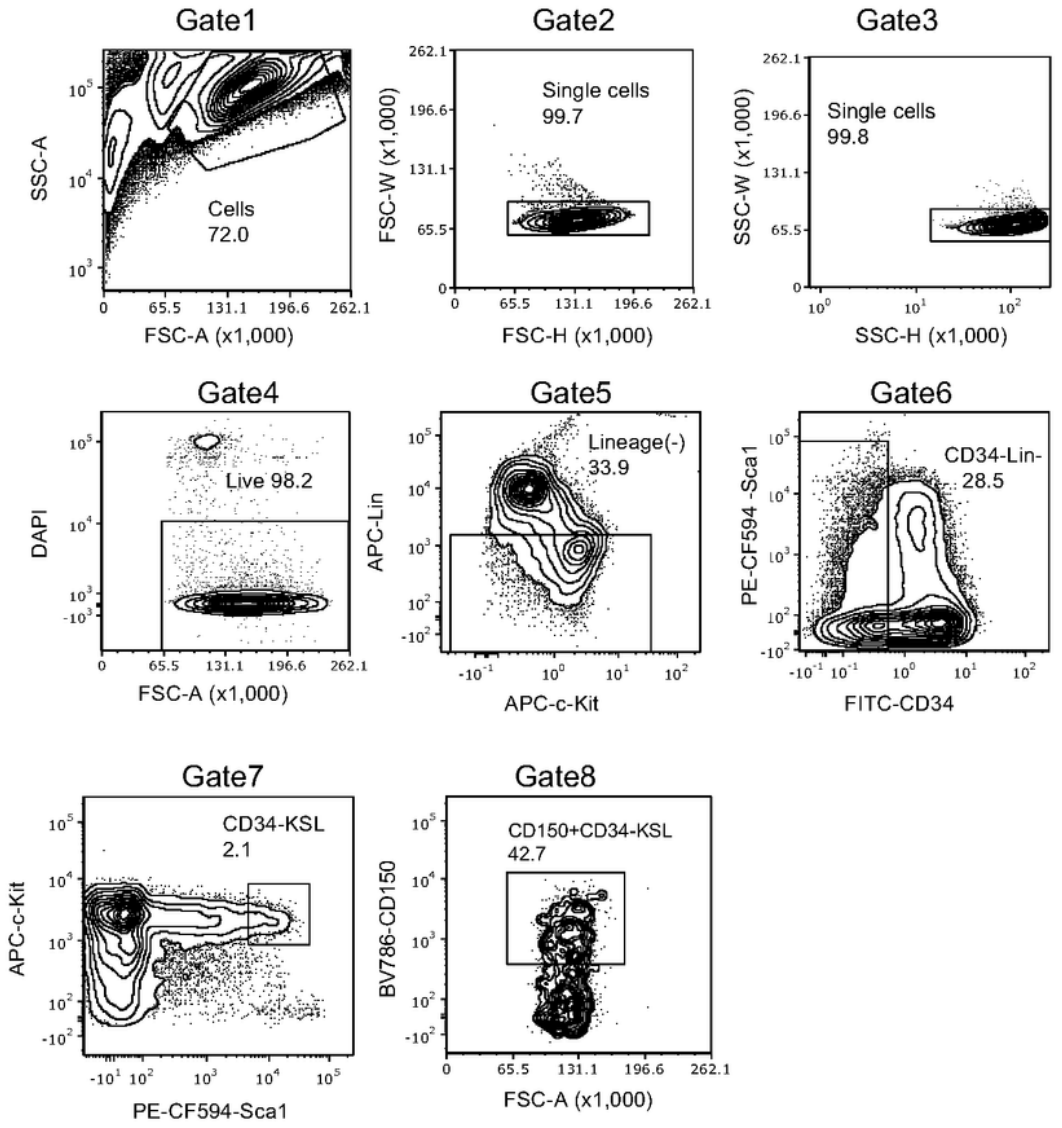

Figure 1

Representative gating scheme for FACS purification of mouse HSCs from young wild type mice. Live CD150 (SLAM)+CD34-Kit+Sca1+Lineage- HSCs were isolated by FACS from c-Kit-enriched bone marrow cells with the gating scheme and directly sorted in fresh HSC complete medium. FSC-A (forward scatter area), FSC-H (forward scatter height), FSC-W (forward scatter width), SSC-A (side scatter area), SSC-H (side scatter height), SSC-W (side scatter width).

Figure 2.

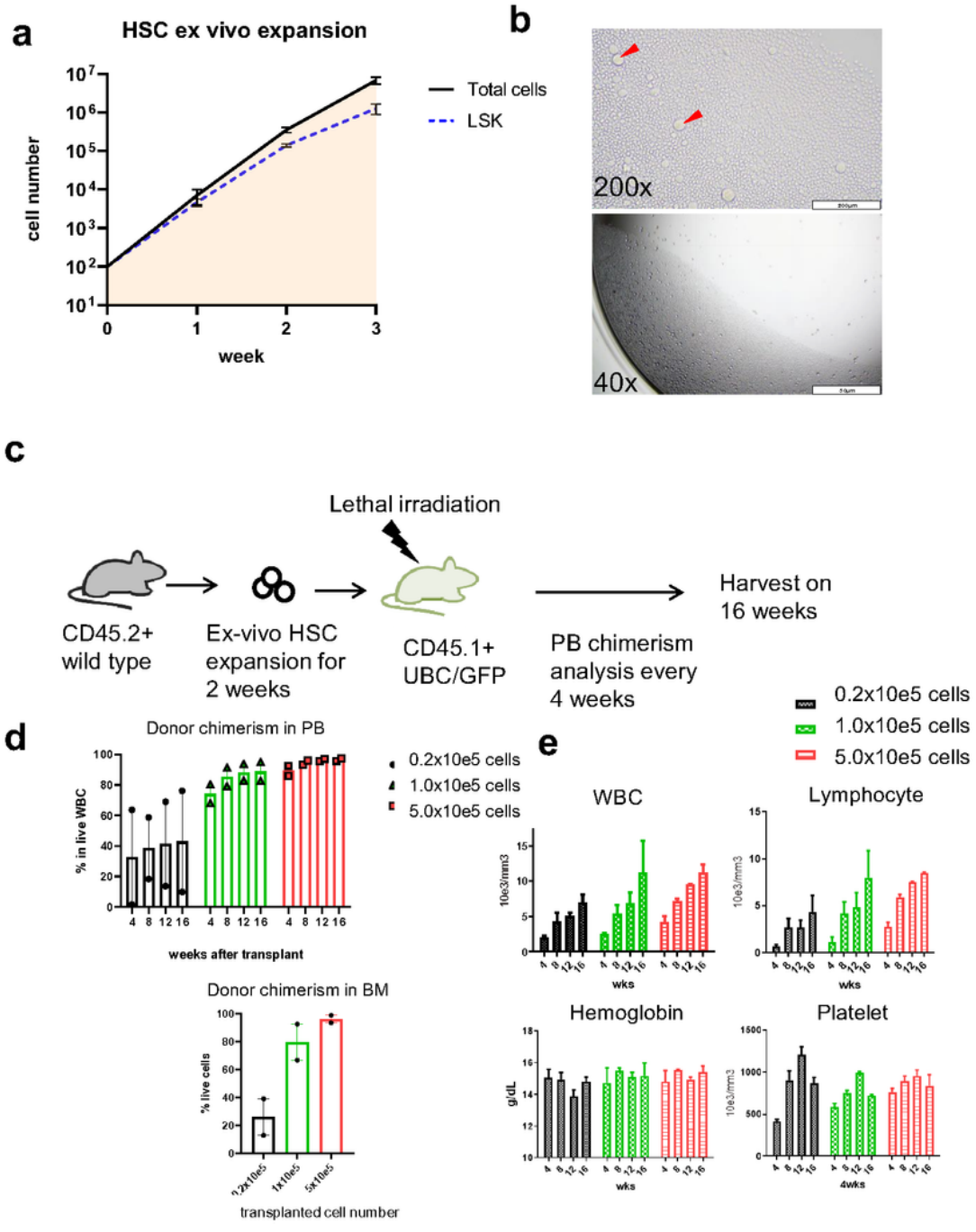

Figure 2

Robust *ex vivo* expansion of HSCs from young wild type mice.

A. The cell number of total cells and KSL (cKit+Sca1+Lineage-) during *ex vivo* culture.

Total cell number was manually counted and KSL cell number was evaluated from flow cytometry. Data represent mean± SEM from three independent experiments. B. The representative images of *ex vivo* HSC culture. The cells expanded in 96-well fibronectin coated plate and the images are expected cell density on day 11 at 40x and 200x magnification. C. Scheme of the noncompetitive transplant of *ex vivo* HSC donor cells into recipient mice with lethal irradiation. HSC cells were purified from CD45.2BL6 bone marrows and expanded in vitro for 2 weeks. Cells were injected into CD45.1 UBC/GFP mice after the 12 Gy of irradiation. The donor cell numbers were titrated in three groups ($0.2x10^5$, $1x10^5$, and $5x10^5$ donor cells per recipient). The chimerism in peripheral blood (PB) was evaluated with flow cytometry every 4 weeks, and then recipient mice were harvested in 16 weeks to analyze the bone marrow cells. D. The chimerism of donor cells in PB at 4, 8, 12 and 16 weeks post-transplant, and in bone marrow on 16 weeks (n=2 recipients per group). E. CBCs of recipient mice. Mice were bled to assess CBCs every 4 weeks after transplant.

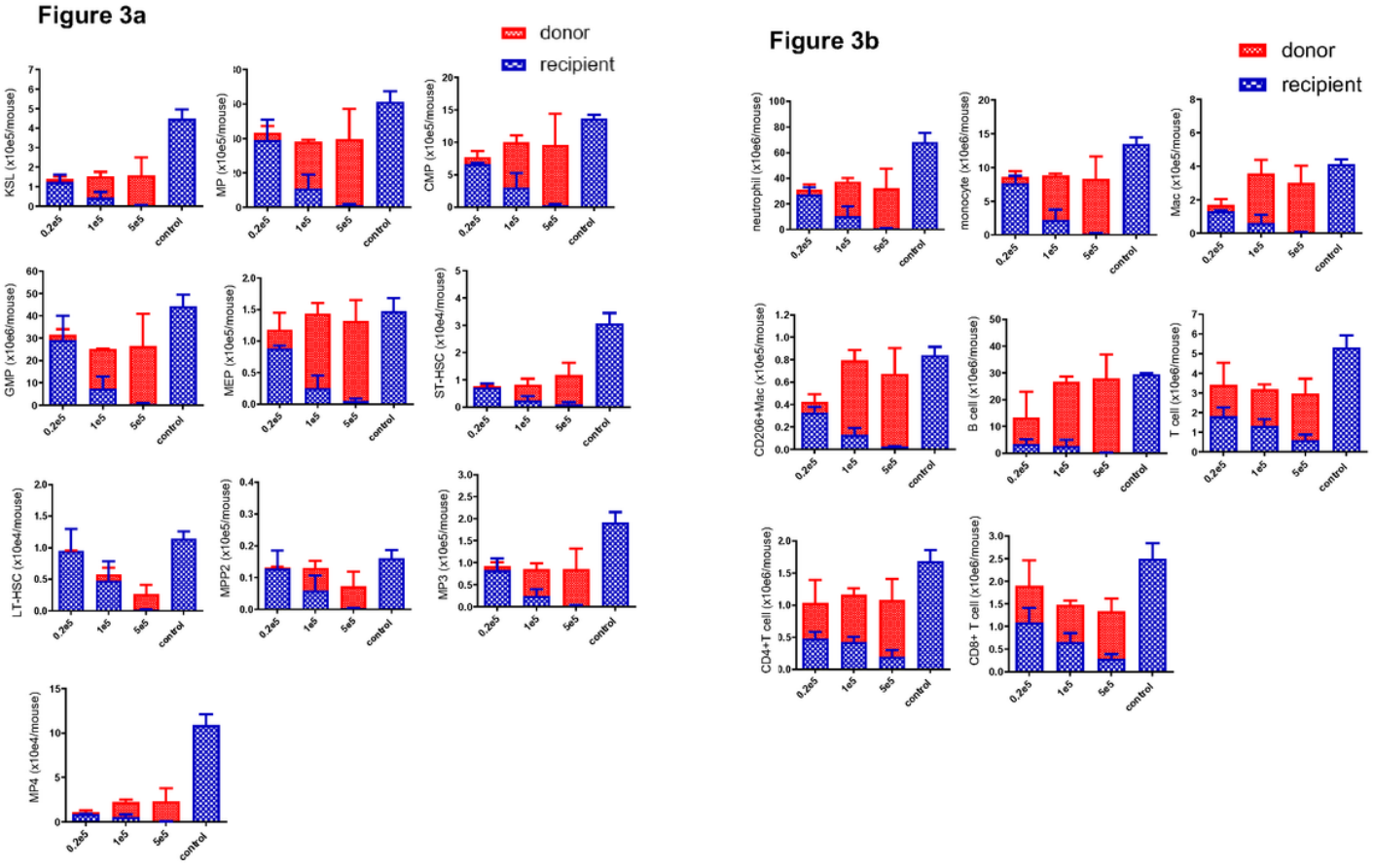

Figure 3

Donor cell dose-dependent contribution to bone marrow HSPCs for *ex vivo* expanded HSCs. Donor cell titration was performed ($0.2x10^5$ cells, $1.0x10^5$ cells, and $5x10^5$ cells per shot for lethal irradiated recipients) A. The absolute number of donor or recipient cells in each HSPC population. B. The mature cell number of donor or recipient cells. Control mice were not irradiated and matched with age and sex as recipient mice. Red highlighted is donor and blue highlighted is recipient cell determined with flow cytometry. MP (myeloid progenitors)($Lin^-/c\text{-}Kit^+/Sca1^-$), CMP (common myeloid progenitor) ($FcγR^-/CD34^+$), GMP (granulocyte-macrophage progenitors)($FcγR^+/CD34^+$), MEP (megakaryocyte-erythrocyte progenitors)($FcγR^-/CD34^-$), ST-HSC(short term-HSC)($KSL^+CD150^-CD48^-Flt3^-$, LT-HSC(long term-HSC)($KSL^+CD150^+CD48^-Flt3^-$).

Figure 4.

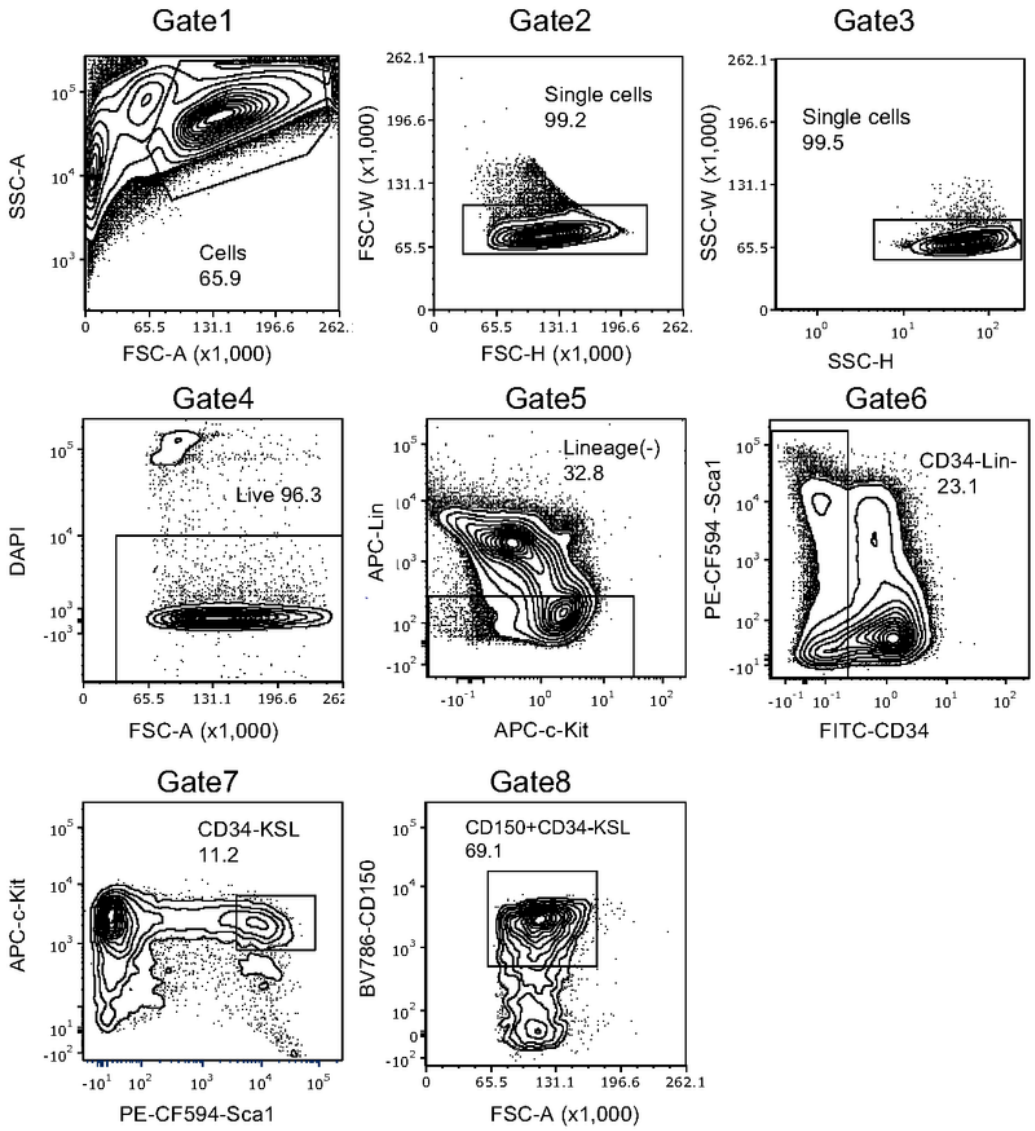

Figure 4

Gating scheme for FACS purification of bone marrow HSCs from aged MNX mice. Live CD150 (SLAM)$^{+}$CD34^{-}Kit^{+}Sca1^{+}Lineage^{-}HSCs were isolated by FACS from pooled bone marrow cells from MNX aged mice as described above.

Figure 5.

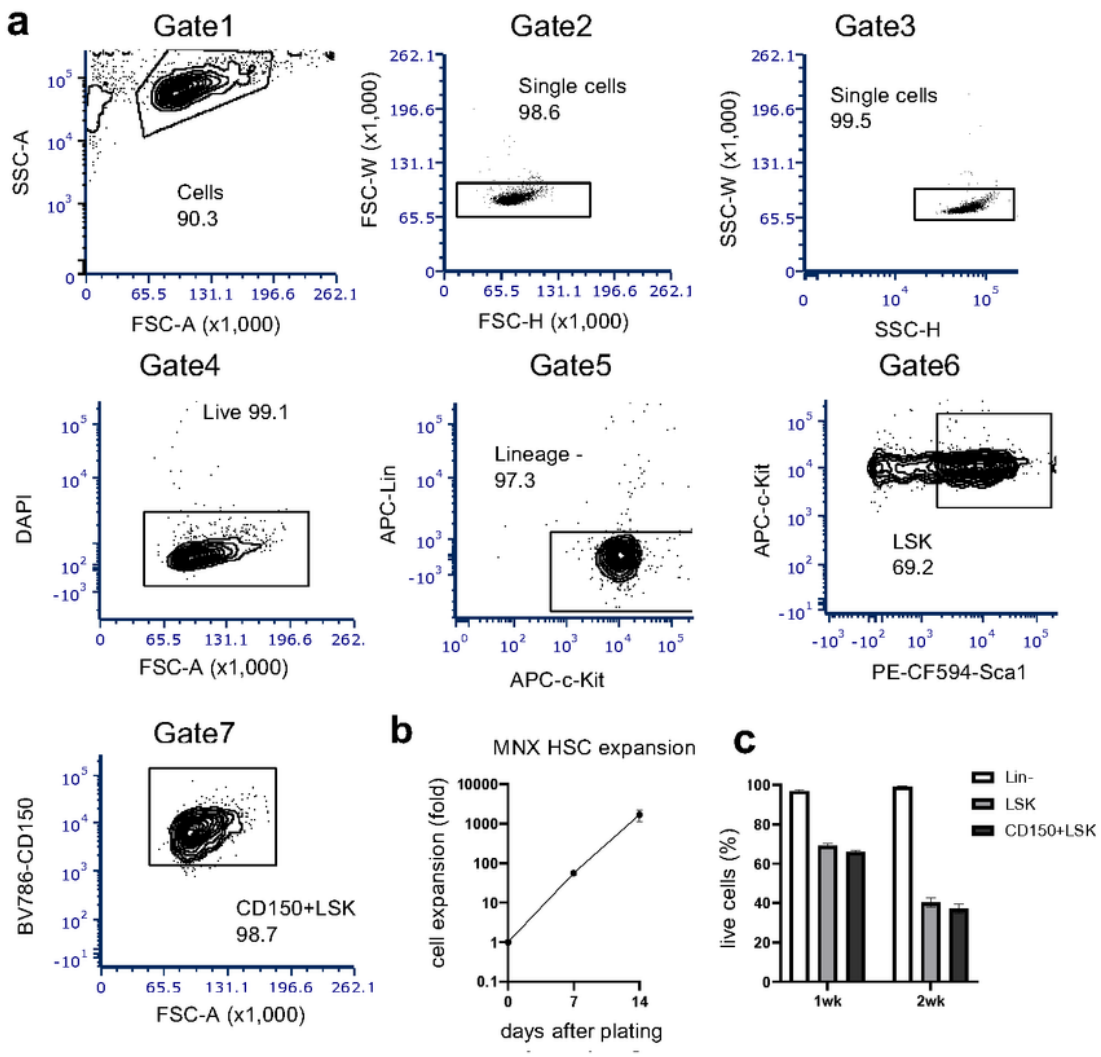

Figure 5

The representative gating scheme of quality check for *ex vivo* HSCs from MNX aged mice bone marrows. A. HSC cultures were analyzed by flow cytometry using the gating scheme as shown on day7 after sorting HSCs. B. Cells expanded *in vitro* HSC culture were counted every week. C. The quality check was performed every one week until the transplant day from duplicate well. Lin- (lineage negative), KSL (cKit+Sca1+Lineage-).

Figure 6.

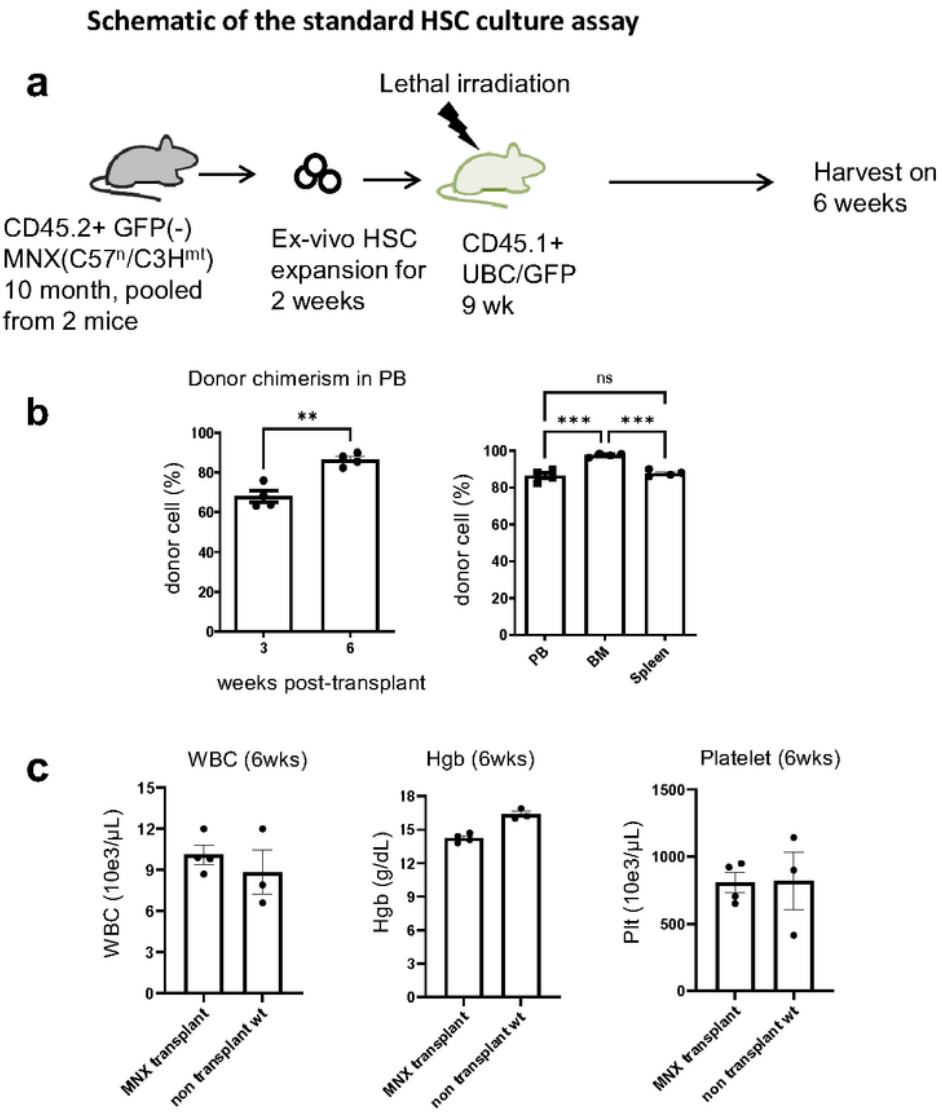

Figure 6

Functional assay of *ex vivo* expanded HSCs from aged MNX mice utilizing transplant model. A. Schematic of the MNX experiment. CD150+CD34-KSL HSCs purified from CD45.2+GFP(-) MNX mice were expanded for 14 days and then transplanted into 4 lethally irradiated recipient mice without any

competitors. Each recipient received 5x10^5 cells. B. Donor chimerism of donor cells of live white blood cells in peripheral blood, bone marrow, and spleen on 3 or 6 week (harvest day). C. Complete blood counts on 6 week. Non-transplant wild type mice were matched age and sex with recipient mice and were not irradiated and. Each dot represents an individual mouse. Values are the means±SEM. One-way ANOVA, Tukey post-hoc test.

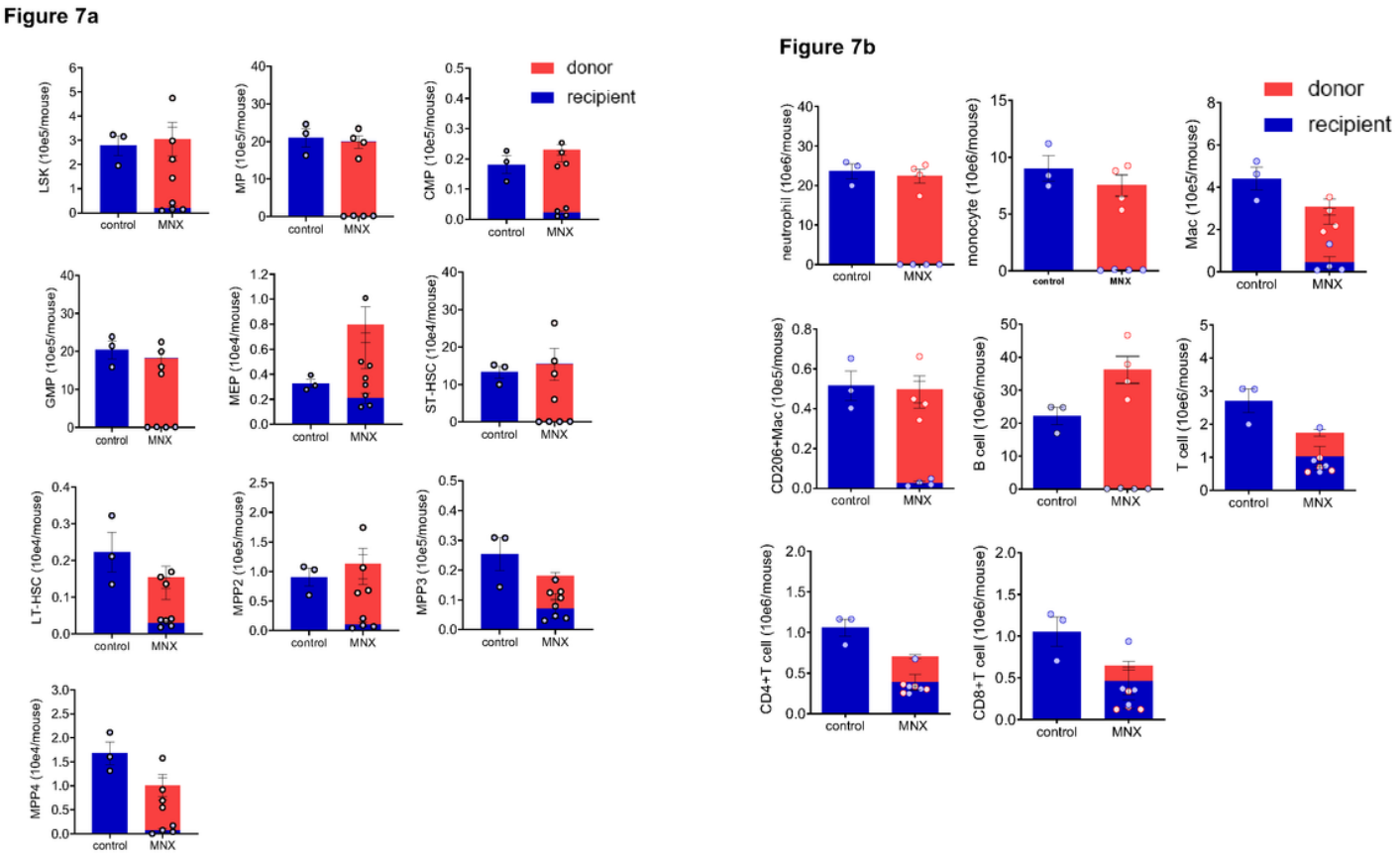

Figure 7

The composition of bone marrow cells in recipient mice transplanted by donor HSCs from MNX mice. Donor cells (5x10^5 cells per shot) were injected in lethal irradiated recipients. A. The absolute number of donor or recipient cells in each HSPC. B. The mature cell number of donor or recipient cells. Control mice were not irradiated and matched with age and sex as recipient mice. Red highlighted is donor and blue highlighted is recipient cell determined with flow cytometry.

Figure 8.

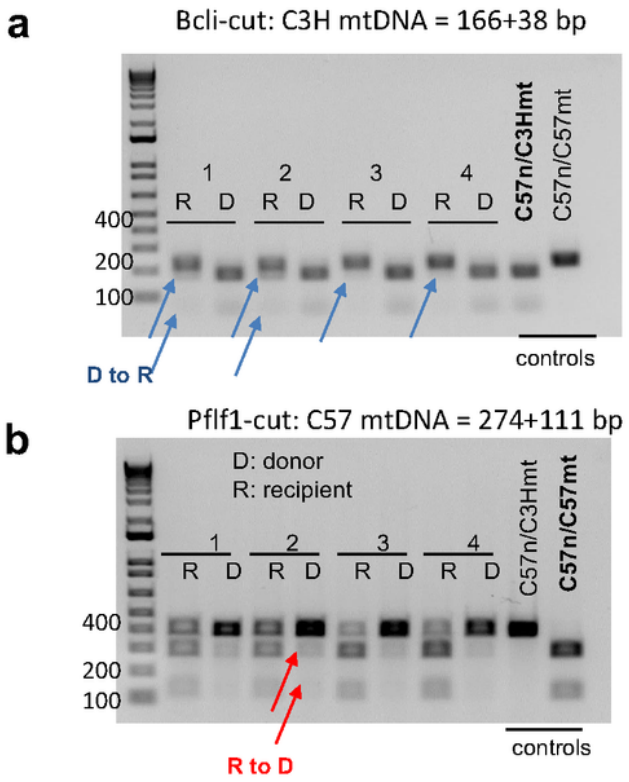

Figure 8

The mitochondrial DNA analysis in separated donor and recipient spleen cells. A. Analysis of C3H mtDNA with *Bcl1*-cut in recipient (R) or donor (D) cells. D to R indicates mitochondrial transfer from donor to recipient. C57 mtDNA evaluation with *Pflf1*-cut in each cell population. R to D indicates the reverse mitochondrial transfer from recipient to donor. Blue arrows indicate evidence of donor to recipient

mitochondrial transfer. Red arrows indicate recipient to donor mitochondrial transfer. Each set of bands represent an individual mouse.

Supplementary Files

This is a list of supplementary files associated with this preprint. Click to download.

- supplementaltableS1.pptx